

# Molecular detection of Dengue Virus using optomagnetic detection technology and centrifugal microfluidics

Catarina Lourenço Nogueira<sup>1</sup>, MSc in Biomedical Engineering  
MEBiom, catarina.nogueira@tecnico.ulisboa.pt  
Supervisors: Marco Donolato <sup>2</sup>; Prof. João Pedro Conde <sup>1</sup>

<sup>1</sup> Instituto Superior Técnico (IST), Universidade de Lisboa, Lisboa, Portugal

<sup>2</sup> Blusense Diagnostics, Copenhagen, Denmark

November 2016

## Abstract

Dengue and Zika virus are nowadays a major public health concern. Within the last 50 years, incidence has increased 30-fold, estimating that 50-100 million infections appear annually. These viruses are transmitted by *Aedes* mosquitoes, found in tropical/subtropical countries. In these poor-resource regions, conditions for expensive diagnostic and preventive protocols are defective. Hence, there is great demand for sensitive, cost-efficient and point-of-care biosensor technologies, capable of detecting virus at molecular level.

Loop-mediated isothermal amplification is a powerful molecular technique, highly specific for a DNA/RNA sequence. It is demonstrated for the first time, in this work, integration of this amplification method with optomagnetic biosensor technology, and incorporation in a centrifugal microfluidic system to realize a low-cost point-of-care platform for molecular detection.

This project, in collaboration with Denmark Technical University and Blusense Diagnostics, a biotech start-up, initiated the development of optimized protocols for detection of viruses, using end-point assessment and real-time monitoring of LAMP reaction. It is shown that after 30 minutes, the end-point amplification assay allows detection of down to 100aM of Dengue-2 synthetic target, corresponding to 6000 molecules of viral DNA, in 30 $\mu$ L total volume. Moreover, a Real-Time approach was implemented, where within 20 minutes of reaction it is possible to detect 300aM of Dengue-2 DNA, in 100 $\mu$ L of LAMP mixture.

Furthermore, extracted RNA viral samples detection is validated using this readout, which together with a microfluidic design for sample splitting, paves the way to fully incorporate genomic extraction, sample preparation, reaction and detection for virus differentiation in low-cost multifunctional systems.

**Keywords:** Dengue Virus, Point-of-care Diagnostics, Loop-mediated Isothermal Amplification, Magnetic Nanoparticles, Centrifugal Microfluidics

## 1. Introduction

Dengue and Zika are fast spreading mosquito-borne viral diseases. Within the last 50 years, incidence has increased 30-fold and is currently estimated that 50-100 million new infections appear annually. These viruses are transmitted by *Aedes* mosquitoes, typically found in tropical and subtropical countries. They are spreading to new areas, currently putting almost half of the world population at risk. Furthermore, there are known complications associated with these viruses, namely Dengue haemorrhagic fever and birth defects in Zika-infected pregnant women (microcephaly and Guillian-Barré Syndrome)[1].

There are still no treatment options for dengue and there is only one reported vaccine (Dengvaxia), whose administration has started in some of the at-risk or infected countries. Thus, controlling spreading of Dengue and Zika viruses relies mainly on prevention, which depends highly on vector mosquito control measures and on diagnosis for epidemiological containment [1].

Early detection of the viral infection is therefore very important during possible outbreaks. Since the first sign of Dengue and Zika is its presence in blood, molecular based approaches, where the virus or its genome are targeted, become an attractive method for detection of these virus. Also, molecular meth-

ods are more specific since they are based on the DNA/RNA sequence of the target. For this reason, they allow better distinction between Dengue and Zika virus than standard serological assays, which suffer from strong cross-reactivity.

Current molecular diagnostics include Reverse Transcriptase Polymerase Chain Reaction (PCR) or Nucleic Acid Sequence Based Amplification (NASBA) [2]. However, these methods require expensive systems, infrastructure laboratories, costly reagents and specific training.

Loop-mediated isothermal amplification (LAMP) is an isothermal technique, which decreases the need for some of the apparatuses needed for standard molecular amplification methods, it has exponential efficiency and is highly specific for a particular DNA/RNA sequence. Therefore, it becomes a desirable technique for detecting and possibly differentiating viruses.

Furthermore, tropical infectious diseases typically stand for poor-resource countries where conditions for expensive diagnostic and preventive protocols are defective. In those regions, there is great demand for sensitive, cost-efficient and point-of-care (POC) biosensor technologies. Thus, in the present work, the detection Dengue and Zika virus will be validated with LAMP method and using a simple, low-cost optomagnetic readout.

## 2. Background

### 2.1. Loop-mediated Isothermal Amplification

LAMP is a powerful amplification technique which is highly specific for a particular DNA/RNA sequence. It shows high efficiency and has the major advantage over other amplification techniques of operating under isothermal conditions, which is possible by the use of an enzyme (polymerase) with high strand displacement activity at a range around 67°C [3].

When designing LAMP experiments, 4 primers are required to recognize different regions in the target DNA/RNA sequence. Amplification starts from strand invasion by one of the inner primers (FIP), while DNA polymerase separates the target DNA duplex and expands the primers. Then, this product gets displaced, this time by an outer primer, which anneals to an upstream target region. At this stage, a self-hybridizing loop structure is formed, which in turn is again displaced and annealed, resulting in a dumb-bell like structure with multiple sites for primers to bind and start LAMP amplification. The resulting products of LAMP reaction are amplicons with various sizes and multiple loops, and magnesium pyrophosphate, a white insoluble precipitant. [4, 5, 6, 7].

In the literature it is widely discussed the contamination issues associated with LAMP, due to

its exponential amplification capability. Nonetheless, a well accepted approach [8, 9, 10] has recently emerged based on the use of (Uracil-DNA-Glycosylase) UDG and (Deoxyuridine Triphosphate) dUTP. In short, dUTP is added to the reaction solution, additionally to the standard DNA bases, and is incorporated in the amplicons. Then, before proceeding to the next amplification reactions, the mixture is digested with UDG enzyme, which specifically removes uracil bases, degrading the product of previous reactions while not affecting the target DNA (which only contains thymine and does not contain uracil).

### 2.2. Optomagnetic Readout

The detection system makes use of a uniaxial applied magnetic field generated by two electromagnets ( $B(t) = B_0 \sin(2\pi ft)$ ), a 405nm laser light source (with direction parallel to the applied field), and a photodetector, with the magnetic nanoparticle (MNP) solution placed between them, as illustrated in **Figure 1**.

The optomagnetic readout principle is then based on optical measurement of rotational dynamics of MNPs and its influence on modulation of light's intensity, in terms of its change in amplitude, phase or polarization of the radiated oscillations. Light scattering effects by dispersed MNPs in solution are the primary cause for the change in light's harmonic composition before and after passing through the MNPs solution, and are mainly observable in the complex second harmonic [11].

The photodetector signal is measured using a lock-in amplifier, which allows for extracting the modulation of the optical signal exactly at the same magnetic field excitation frequency [11]. The measurement is composed of a series of sweeps at different frequencies and the output is constituted by the frequency, in-phase and out-of-phase components of the second harmonic ( $\Re(V_2)$  and  $\Im(V_2)$ ), extracted from the Data Acquisition Unit and lock-in amplifier. The range of frequencies used (typically from around 3000Hz to 1Hz) allows characterization of the whole MNP dynamics.

When a uniaxial magnetic field is applied, for a single superparamagnetic particle, its magnetic moment tends to align with the field so as to minimize the energy, while after removal of the field, their magnetization average nulls. If a time-oscillating field is applied, that same single superparamagnetic MNP will rotate inside the particle following the external field variation [11].

In contrast, a different scenario occurs for larger size magnetic particles or for bound together MNPs. Here, they do not exhibit that switch on-off performance and instead, after removal of an applied magnetic field, there is a remnant magnetic moment. If this happens, a dipole magnetic moment is created

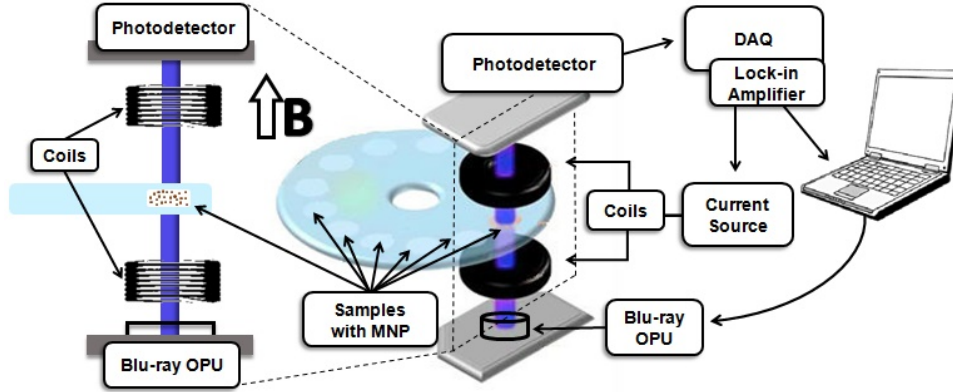


**Figure 1:** Schematic illustration of the optomagnetic readout set-up used in the approach described in this study.

and the external magnetic field can induce a torque on the MNPs, which in turn causes their physical rotation (**Figure 2**).

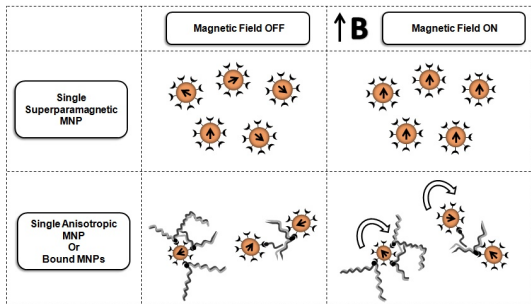


**Figure 2:** Representation of the response to a uniaxial magnetic field for single superparamagnetic MNPs, anisotropic MNPs with remnant moment and clusters of MNPs.

The MNPs used in this study have a behaviour close to superparamagnetic. However, they still exhibit a remnant moment. This means that the external field can exert a torque even on individual particles, which then rotate under the field variation (as illustrated in **Figure 2**).

On this account, there is a clear frequency dependence on the optomagnetic signal from the MNPs. In the lower frequency range, the response is in-phase with the magnetic field excitation. A phase lag will appear compared to the excitation when frequency is increased until a peak in  $\Im(\chi)$  appears, which corresponds to a zero in the  $\Im(V_2)$  signal. The frequency at which this happens is called Brownian relaxation frequency ( $f_B$ ) and is given by the formula presented below [11].

$$f_B = \frac{k_B T}{6\pi\eta V_h} \quad (1)$$

From the formula it is possible to observe a correlation between the peak frequency and the hydrodynamic volume of the particles ( $V_h$ ), since larger par-

ticles tend to rotate out-of-phase at lower frequencies in comparison with smaller particles, which is illustrated in **Figure 3**.

Taking a look at the positive sample, the functionalized single MNPs are bound to higher volume molecules in comparison to the negative control. It is intuitive to understand that for higher hydrodynamic volumes, the particles will rotate slower in response to magnetic field.

For instance, if larger amounts of DNA, after being amplified, are bound together with a MNP, the particle will physically rotate much slower, contrary to a control, where the MNPs are only bound to small size primers, as exemplified in **Figure 3**. Therefore, they will exhibit lower values for the Brownian relaxation frequency (frequency at which the peak is located).

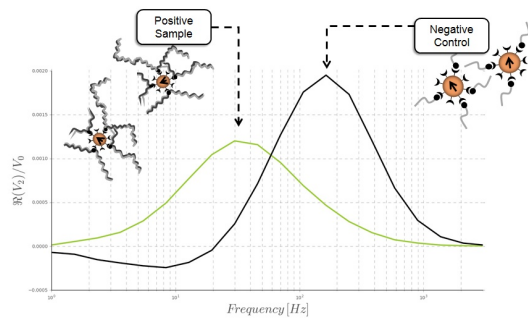


**Figure 3:** Representation of the difference in  $\Re(V_2)/V_0$  for solutions of MNPs with different hydrodynamic volumes.

The optomagnetic detection principle is based on the combination of LAMP products with functionalized MNPs.

One of the primers (FIP) is biotinylated, which results in production of amplification products which have incorporated biotin in its constitution and can be of variable sizes. MNPs are functionalized with a molecule that is known to form strong bonds with biotin, which is streptavidin. Therefore,

they have multiple sites on their surface for this connection to form and the final solution is composed of dispersed individual MNPs attached to the LAMP products.

### 2.3. Centrifugal Microfluidics

With reduced amount of instrumentation, centrifugal microfluidic systems only require a compact motor to create the forces for liquid manipulation as opposed to the standard use of external syringe pumps [12, 13].

Fluid dynamics in these systems relies on centrifugal forces to drive fluids across channels and chambers, depending on their geometry and radial position, on the rotational speed imposed, and on the fluidic properties, such as viscosity and density [13].

There are five main forces acting on a liquid element in a rotating disc. Centrifugal force is responsible for the centripetal acceleration driving the fluid towards the edges in the radial direction. Coriolis force is generated when the liquid has a radial component of velocity and for high enough rotation speed, is the major force driving the fluid and the Euler force is the response to any difference in angular acceleration. Moreover, viscous Stokes drag is a frictional force which accounts for the fluid's viscosity and if suspended particles or gas bubbles are present, they experience a sedimentation force under the impact of a centrifugal force [12].

One important feature to pay attention to is the dependence on the frequency of rotation  $\omega$  for the aforementioned forces, which therefore serves as a fundamental parameter in controlling fluid motion.

Besides outwards radial movement from the centre to the edge of the disc, by controlling the rotation rate and design of the microfluidic structures, several other fluidic functions may be integrated, allowing the production of more complex systems. These include valving, volume metering, calibration, liquid mixing, sample splitting and fluid separation [12, 13].

## 3. Materials & Methods

### 3.1. Microfluidic Design & Production

All cartridge and disc designs were drawn in Computer-aided Design (CAD) software tools (either SolidWorks or DraftSight), which were then either cut using a  $CO_2$  laser or milled and hot embossed. The polymer material used was Poly(methyl methacrylate) (PMMA), and the used discs to be cut were of the following thicknesses: 0.6mm, 1.2mm and 2mm.

The  $CO_2$  laser (EPILOG laser, Model Zing 16) allows rapid patterning of discs by guiding a laser in the X-Y plane to cut the structures imported from the CAD designs in a PMMA disc. Similarly, the sketches obtained from SolidWorks were transferred

to the milling machine (Minitech CNC Mini-Mill, Minitech Machinery Corporation) for production of an aluminum negative master. After, the aluminum plate and a PMMA disc were put in a hot embosser (25T hydraulic lamination hot press, MTI Corporation), which produces the features while maintaining the polymer microstructure.

The microfluidic discs used typically have between 3 and 5 layers, which means that alignment and bonding of layers were critical factors. To satisfy them, alignment holes were included in every layer, so that after obtaining the discs with desired structures, it was possible to correctly assemble the layers using pins. To ensure correct bonding, assembly of discs was done using a Pressure-sensitive Adhesive Tape (PSA), providing the necessary adhesion between layers and then the resulting disc was rolled in a laminator (Mega Drive Laminator, Mega Electronics Ltd) to further decrease the probability of liquid leaking.

### 3.2. Biochemical Materials & Protocols

LAMP molecular amplification inherently requires the following reagents in the initial mixture: primers' mixture (combining the primers FIP, BIP, F3, B3, LF and LB, obtained from DNA Technologies); isothermal amplification buffer (Contains Tris-HCl,  $((NH_4)_2SO_4$ , KCl,  $MgSO_4$ , Tween<sup>®</sup>20 and a pH of 8.8 at 25 °C obtained from NEB - New England Biolabs); extra  $MgSO_4$  (NEB); *Bst* Enzyme (NEB); solution with the target DNA or RNA sequence (from Integrated DNA Technologies).

Furthermore, to enable optomagnetic detection, 100nm streptavidin-coated multicore bionized nano-ferrite magnetic nanoparticles were added to the reaction mixture above (purchased from Micro-mod Partikeltechnologie).

dUTP and UDG enzyme used in the UDG-LAMP method were purchased from Affymetrix and the integration of colorimetric approach with molecular amplification procedure was based on the use of Eriochrome Black T dye (from Sigma Aldrich).

The Dengue and Zika Virus synthetic targets were taken from previous studies ([14] and [15]), while for *E.coli* bacteria were designed by a collaborator. These target sequences were all purchased from Integrated DNA Technologies. Furthermore, inactivated Dengue-2 virus strain 16881 vero cells (Meridian Life Science) were obtained in order to validate the chosen primers' sequences.

With respect to experimental protocol, at the beginning of each day, UV exposure to the materials used was done to possibly degrade amplicons. The pre-LAMP mixture containing all necessary reagents was prepared and loaded in the chips in a Laminar Flow Cabinet (LAF) bench in a separate lab of the one used for reaction/detection of amplification products.

### 3.3. Readout Systems

Readout systems used in this work are kept confidential due to company policy.

## 4. Results

Data analysis was performed based on the second complex harmonic, since it is where modulation of light is mainly observed. More specifically, an increase in the hydrodynamic volume of the MNP bound to the amplification products leads to a shift in frequency for the peak observed for  $\Re(V_2)$  towards the lower frequency range.

When presenting the in-phase and out-of-phase signals for the second harmonic, they were normalized by simultaneously measured values of zero harmonic  $V_0$  to compensate for variations in intensity of the light and reflection and/or absorption in the chips as well as to account for changes in transmittance due to chips' production variability.

In order to find the frequency correspondent to the peak of  $\Re(V_2)/V_0$ , an algorithm was developed in Python which based on the maximum value of a 2nd order polynomial fitting of the in-phase values with respect to frequency range.

### 4.1. End-Point (EP) LAMP

In the first stages of amplification experiments, the synthetic target used was *E.coli*. It was examined the dependence of the LOD and dynamic range on the reaction duration (20 and 25 minutes), setting the temperature at 67°C (data not shown).

Loss of dynamic range with increasing reaction durations was confirmed. Moreover, a LOD of 10aM was achieved with 20 minute reaction, as opposed to 25 minutes (30aM), which was not in accordance with the expectation that higher reaction times lead to the detection of lower target concentrations.

However, the system did not exhibit good reproducibility for such small volumes and the number of repetitions carried out for each concentration is not high enough to be considered statistically relevant.

#### 4.1.1 Influence of MNPs concentration

The previous experiments served as a validation model of the methodology of integration of LAMP on chip using optomagnetic detection as well as it allowed familiarization with the technique. After, the amplification protocol was modified so as to detect Dengue subtype 2.

Before trying to obtain a dose response curve based on peak frequencies for the range of target concentrations 300pM - 10aM, a comparative analysis was carried out in terms of MNPs' concentration. There is no doubt that modulation of light intensity by individual MNPs is highly dependent on their concentration in solution. Hence, EP - LAMP was performed using two more concentrations than the 0.3mg/ml normally used in this work: 0.1mg/ml

and 0.6mg/ml.

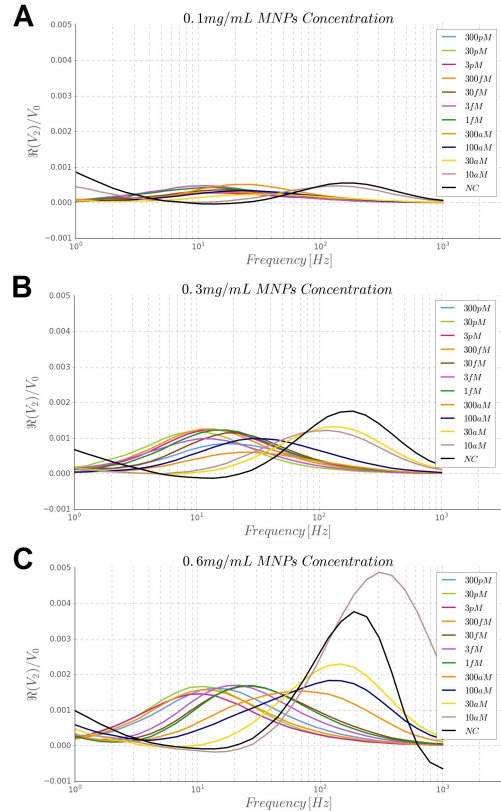


**Figure 4:** Comparison between optomagnetic signal for different MNPs concentrations for Dengue-2 synthetic target. LAMP was allowed to react for 30 minutes at 67° C. Three repetitions of each serial dilution concentration was done to provide statistics for the dose response. A - 0.1mg/ml MNP concentration. B - 0.3mg/ml MNP concentration. C - 0.6mg/ml MNP concentration.

Similar to what has been previously demonstrated [16], an increase in MNPs' concentration leads to detection of higher values in the magnitude of  $\Re(V_2)/V_0$ . (**Figure 4**) The explanation for this phenomena lies in the fact that, as more modulating units are present in solution, the intensity of light is more severely modulated and higher signal is obtained.

Data shows that the amount of MNPs influences tremendously the sensitivity of this assay. The focus of this approach is on the signal received from individual MNPs therefore them binding together forming aggregates is undesirable. For higher concentrations of MNPs, the probability of agglutination is larger since there is higher amount dispersed in solution, which increases the chances of unspecific MNPs binding to each other.

Thus, higher MNP concentration leads to more background noise but increases the number of modulating units that are bound to amplification prod-

ucts and lower MNP concentration increases sensitivity but decreases the chances of MNPs meeting the target.

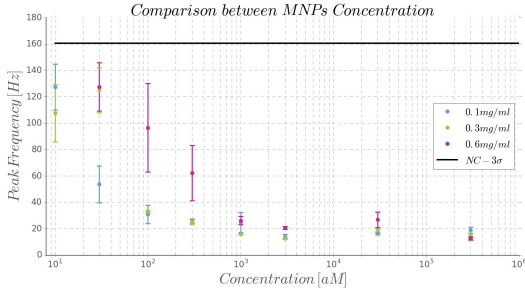


**Figure 5:** Peak frequency plots with respect to concentration for the different bead concentrations used. Blue, green and pink correspond to 0.1, 0.3 and 0.6mg/ml concentration. The error bars are the result of one STD calculated from triplet experiments.

In **Figure 5**, it is observable a decrease in the dynamic range with lower MNPs concentration.

It was estimated that a solution with  $1\text{mg}/\text{mL}$  100nm MNPs and  $130\text{nM}$  biotinylated FIP primer results in capturing of approximately 100 DNA molecules per MNP. In these conditions, the decrease in dynamic range can be explained due to the fact that with less MNPs available, more easily a saturation state is obtained where they are all bound to the amplification products.

#### 4.1.2 UDG-LAMP

Not long after the beginning of experiments with *E.coli*, false positives began to appear. Therefore, before changing target to Dengue-2, alternative methods to do LAMP were analysed in order to stop carryover contamination. The method proposed by [17] was implemented (where dUTP and UDG enzyme is added additionally to the reaction mixture).

**Figure 6** and **7** show the results for LAMP done at  $67^\circ\text{C}$  for 30 minute reaction, with a MNP concentration of  $0.3\text{mg}/\text{ml}$ . In terms of LOD, the lowest detectable concentration is  $100\text{aM}$ . Knowing that one molecule of DNA corresponds to one virus particle, it was estimated that this amount corresponds to 6000 molecules of virus synthetic DNA. Moreover, it is clear from **Figure 7** a linear relation in the range of concentrations  $100\text{aM} - 30\text{fM}$ .

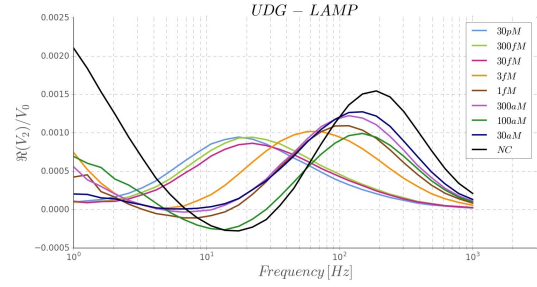


**Figure 6:** Average  $\Re(V_2)/V_0$  signal obtained from UDG-LAMP in the  $30\text{pM} - 30\text{aM}$  concentration range. The average signal was the result of three repetitions for each concentration.

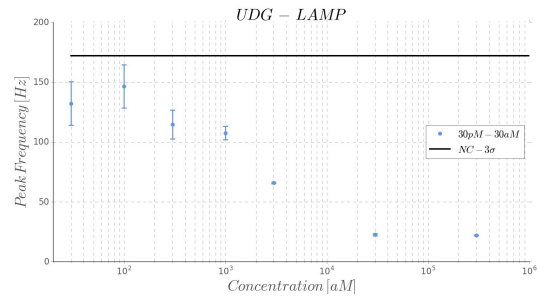


**Figure 7:** Frequency of the peaks with respect to concentration of target, with representation of the negative control in the  $NC - 3\sigma$  parameter. The error bars correspond to one STD from three repetitions experiments for each concentration.

## 4.2. Real-Time (RT) LAMP

Real-Time (RT) measurements allow better understanding of the kinetics of LAMP reaction by enabling continuous monitoring of the optomagnetic signal received by the photodetector. It provides exclusive insight into the kinetics of the reaction, in view of understanding when amplification begins, rate of reaction and when a saturation state is achieved. Data processing and analysis for this section was performed similarly as for **End-Point LAMP**.

### 4.2.1 Parameter Optimization

First of all, taking advantage of the valuable information taken from RT measurements, further examination on the influence of several parameters, such as temperature, magnesium concentration and kinetics of the UDG method, were carried out.

Three experiments using the same target concentration were carried out under three different temperatures,  $67^\circ\text{C}$ ,  $68^\circ\text{C}$  and  $69^\circ\text{C}$ .

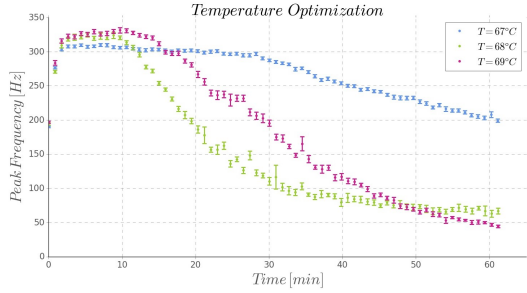


**Figure 8:** Comparison between different temperatures for RT LAMP set up (67°C, 68°C and 69°C).

The results are presented in **Figure 8**. At a first sight, one might choose to set 68°C in the protocol for future experiments. However, higher temperatures give greater chance of destabilizing weak bonds and possibly slowing down contamination. For this reason, 69°C was the preferred choice for the rest of experiments done for the detection of Dengue-2 synthetic target.

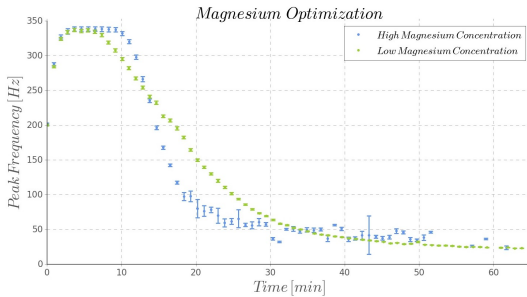


**Figure 9:** Optimization of magnesium concentration for RT-LAMP in terms of reaction velocity and noise in the signal.

For the sake of further examining dependence of magnesium ion in LAMP, two concentrations were used (**Figure 9**). As mentioned before, there is a range of values in which the assay will work, but for higher values in which the appearance of false positives is promoted (amplicons from previous reactions are stabilized in the solution) and for lower the *Bst* enzyme might not be fully functional. More than that, higher amounts of the ion originate more noisy results due to the enhanced production of magnesium pyrophosphate.

These factors can be identified in the graph on account of decreased slope (velocity of the amplification) and noise for the lower concentration of magnesium.

#### 4.2.2 UDG-LAMP

dUTP base and UDG enzyme were included in the protocol for reaction to further investigate whether this method was efficient in stopping contamination.

Moreover, thymine was completely replaced by uracil base. Since RT-LAMP took longer reaction durations, it allowed more conclusive analysis on whether uracil was incorporated. Even if this base took much more time than thymine to be used for production of amplicons, one would expect to observe a start in frequency shift.

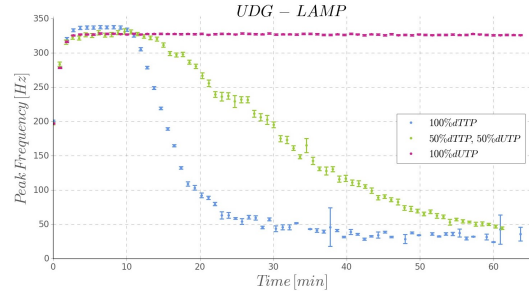


**Figure 10:** Comparison between different concentrations of dUTP and dTTP in RT-LAMP.

For 60 minutes of reaction (which was much more time needed for reaction for even the lowest target concentrations), **Figure 10** shows no shift for the sample with 100%dUTP, contrary to the ones that included dTTP, indicating that there was no guarantee uracil base was actually being incorporated in the amplicons during LAMP reaction.

Furthermore, standard LAMP (100%dTTP) was compared to UDG-LAMP (50%dTTP, 50%dUTP). Besides the production of amplicons starting at around the same time (10 minutes), the velocity of amplification was diminished when dUTP was included in the solution.

This decrease points out that presence of dUTP slowed down the incorporation of bases in the elongation process, which might be explained by the fact that basically dUTP and dTTP are equivalents in terms of their chemical composition and structure (dTTP has one additional methyl group in the aromatic ring). Thus, they probably competed for being incorporated by *Bst* enzyme.

#### 4.2.3 Dengue-2 Dose Response

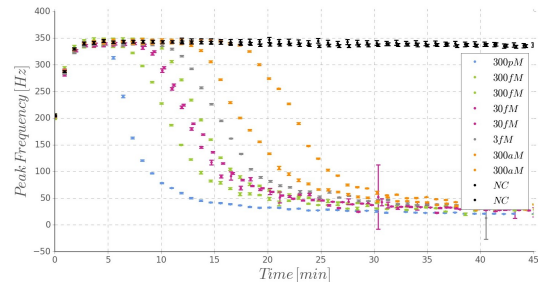


**Figure 11:** Peak frequencies with respect to reaction time using RT-LAMP for the range of concentrations 300pM – 300aM, before contamination has started.

Contamination issues significantly narrowed the possibility to characterize the system in terms of reproducibility, since not many experiments were carried out before the appearance of false positives. Nonetheless, in **Figure 11** there are the RT results for measurements prior to contaminations, where the peak frequency values (found by the same algorithm as for End-Point).

Examining the graph, one can say that all the concentrations exhibit similar velocities of reaction, since the change in peak frequency per period of time is approximately equal (same slope of the curves). Moreover, there is no peak shift for negative control (no contamination) and all concentrations eventually achieved the same final saturation value of frequency.

#### 4.2.4 Extracted RNA of inactivated Dengue-2 virus

With the interest of testing this method for detection of targets closer to real samples, inactivated Dengue-2 virus was purchased, followed by RNA extraction of the molecular content of the virus.

The primers used were the same as for previous studies so it could be possible also to conclude on their specificity for DNA and/or RNA. Furthermore, RNA is known to be more unstable in solution than DNA, so it is also desirable to test its resistance to such higher temperatures, so that in the future the technique can be applied to other viruses.

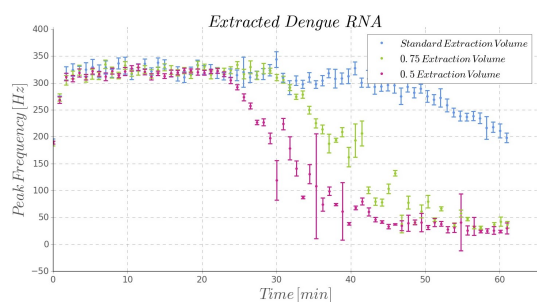


**Figure 12:** Optomagnetic detection of extracted RNA of Dengue-2 inactivated virus with different extraction volumes.

**Figure 12** shows that it is possible to use this optomagnetic readout with the primers designed for synthetic target. Furthermore, RNA extraction was carried out according to the information from the supplier, which had an optimal extraction volume of buffer to dilute the extracted RNA. Still different extraction volumes were used. If a smaller amount of buffer is used for extraction, then the final solution has higher RNA concentration, as observed in the figure.

#### 4.2.5 Zika virus detection

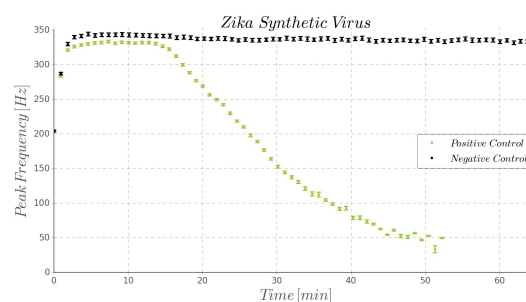


**Figure 13:** Zika synthetic virus detection using RT-LAMP. One negative and one positive control were measured over a duration of 50 minutes at 69°C.

In **Figure 13**, there is proof that this optomagnetic system can detect a high concentration of Zika synthetic virus after approximately 20 minutes at 69°C. The reaction is slower for Zika than Dengue since the slope of the curve is smaller, even though the same protocol was used. Hence, the difference in reaction kinetics between different targets to be detected is noticeable and the need for optimization according to the intended purpose is highlighted.

#### 4.3. Multiplex Cartridge

The ambitious final objective of this work was to incorporate in a single chip differentiation between Dengue serotypes and Zika using LAMP in a low-cost system. Despite not being able to complete this goal, many progresses towards LAMP on a chip have been accomplished.

The main components of both these designs include the chambers for loading of sample, reagents, the final chamber where amplification occurs at the same allowing for optomagnetic readout, and the splitting structure, which accounts for dividing the sample in two equal volumes and transferring it to the reaction chamber.

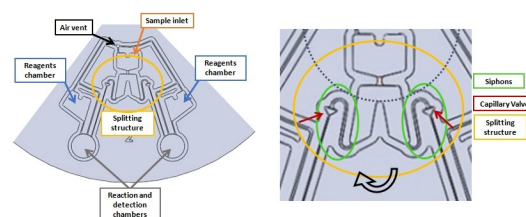


**Figure 14:** Schematic representation of the features of the first design for multiplex cartridge.

From the figures above, it is possible to identify components such as siphons and capillary valves (green and red). After inserting the sample, liquid is spun down to a chamber that is responsible for splitting the volume into two. Assuming that the disc is rotating in the direction represented in

the figure, the right half of this chamber will only be filled after the other one, which means that, after the level of liquid has reached the distal tip of the separation between the two halves. Knowing the initial volume to load, it is possible to sketch this structure so that the sample is equally divided.

Since time is a parameter that highly influences LAMP, it is desirable that the split volumes reach the reaction chamber simultaneously. Thus, while the whole initial volume has not been completely divided, there should be a restraint to the fluid's passage. This is the reason why a siphon is used. By keeping a high enough frequency of rotation, the liquid stays below the crest level. When rotational force is decreased, the siphon is primed and the liquid passes through.

Afterwards it encounters a capillary valve, which allows further control of the moment when the sample reaches the reaction chamber, since below a certain burst frequency, the capillary pressure is higher than the rotational force and the fluid is stopped. However, it should be noted that since the burst frequency is influenced by geometric parameters, namely its distance to the center of rotation. Therefore, it should be made sure that both capillary valves have approximately the same value for this parameter.

The main aspects to keep in mind in both these cartridges is the fact that manipulation of liquids in such structures is deeply dependent on rotational frequency and on the radial distance.

## 5. Discussion & Conclusions

The central objective of this work was to successfully combine several biotechnological fields, namely a molecular amplification technique, a novel optomagnetic readout system and state-of-the-art centrifugal microfluidics.

With this study, further steps were taken towards the development of a low-cost, and sensitive multiplex platform suitable for molecular diagnosis and differentiation of various pathogens. As previously mentioned, these POC systems are meaningful in poor countries, where rapid efficient testing of infectious diseases aids in pandemic containment and resource management in therapeutics.

After completion of this work, an understanding was gained on the complexity of the integration of molecular diagnostics assays into miniaturized POC systems. The number of influencing parameters is vast and affects not only its efficiency, but also its sensitivity and specificity. For instance, there are factors inherent to LAMP technique that were analysed in this work, such as reaction duration, temperature and reagents concentration.

Additionally, several considerations should be made regarding the hurdles encountered throughout this project. The exponential efficiency of this

method produces DNA molecules that easily disperse in the air and attach to surfaces. By doing so, contamination is a constant concern when working with this technique.

Be that as it may, there are still much more factors to explore involved in contamination issues. All isothermal methods tend to produce false positives if kept running for too long. Usually, a cut-off point is set, making a compromise between LOD and encouraging contamination.

Aiming at going lower in target concentrations, one future opportunity might be to change target and to carry out UDG-LAMP with RT monitoring (even without consistent proof that the method is indeed working).

Furthermore, other conceivable changes in protocol include an optimization of factors that are thought to destabilize contaminants in the LAMP mixture. They include an increase in pH (by adjusting the amplification buffer's composition) and heating primers before doing LAMP, which can increase specificity by melting any possible primer multimeres. Furthermore, running a gradient of temperatures, it might be possible to find a small range of temperatures where it is high enough to degrade carry over contaminants (or at least destabilize them enough that they would not bind to primers), and that is below the *Bst* DNA polymerase denaturation value.

Combining LAMP with the use of MNPs in an optomagnetic readout system further increases the complexity of the method. On account of this technique being based on measurements of the modulation of light intensity, configuration of the optical set-up highly affects the optomagnetic signal.

It was demonstrated that MNPs' concentration is correlated with the signal intensity, systems' dynamic range and reproducibility. Lower amounts of MNPs increase the sensitivity of the assay, since they not only saturate with LAMP products much faster, but also the probability of forming aggregates is lower. With respect to agglutination, primer dimers were also found to encourage the formation of aggregates.

Finally, a major challenge in translating molecular diagnostics assays into miniaturized formats compatible with POC settings, lies in multiplexing functions into a single portable system. For this, centrifugal microfluidics have shown to be an advantageous technological field, where instrumentation is reduced and it is less costly. Furthermore, it also enables the development of a complex network that incorporates sample preparation, DNA amplification process and biological detection. In this study, several experiments were conducted to investigate the basic mechanisms behind such technology and to analyse how different microfluidic disc designs

influence the signal outcome.

Comprehension of the physical background behind centrifugal microfluidics allowed the development of a design to perform LAMP, with possible differentiation between virus. Although virus distinction on a single disc was yet not achievable using this molecular amplification process, many steps towards this goal were accomplished.

Overall, it was demonstrated that LAMP reaction is compatible with magnetic nanoparticles for an optomagnetic readout system. A 100aM LOD was achieved for Dengue synthetic target after 30 minutes of detection while also proving the system's ability to detect extracted viral samples. Comparing this system with the common methods for infection detection, while standard approaches might take a matter of days for laboratory testing, using this readout one might expect a positive signal in under one hour.

Future endeavours include a characterization of low-cost systems to perform LAMP on disc with higher sensitivity and doing repetitions for statistical significance for reproducibility analysis. The ultimate goal being integration of the splitting design to perform LAMP for virus differentiation on a single platform.

## References

- [1] W. H. Organization, S. P. for Research, T. in Tropical Diseases, W. H. O. D. of Control of Neglected Tropical Diseases, W. H. O. Epidemic, and P. Alert, *Dengue: guidelines for diagnosis, treatment, prevention and control*. World Health Organization, 2009.
- [2] K. F. Tang and E. E. Ooi, "Diagnosis of dengue: an update," *Expert review of anti-infective therapy*, vol. 10, no. 8, pp. 895–907, 2012.
- [3] X.-e. Fang, J. Li, and Q. Chen, "One new method of nucleic acid amplification: loop-mediated isothermal amplification of dna," *Virologica Sinica*, vol. 23, no. 3, pp. 167–172, 2008.
- [4] T. Notomi, H. Okayama, H. Masubuchi, T. Yonekawa, K. Watanabe, N. Amino, and T. Hase, "Loop-mediated isothermal amplification of dna," *Nucleic acids research*, vol. 28, no. 12, pp. e63–e63, 2000.
- [5] Y. Mori, K. Nagamine, N. Tomita, and T. Notomi, "Detection of loop-mediated isothermal amplification reaction by turbidity derived from magnesium pyrophosphate formation," *Biochemical and biophysical research communications*, vol. 289, no. 1, pp. 150–154, 2001.
- [6] K. Nagamine, T. Hase, and T. Notomi, "Accelerated reaction by loop-mediated isothermal amplification using loop primers," *Molecular and cellular probes*, vol. 16, no. 3, pp. 223–229, 2002.
- [7] N. Tomita, Y. Mori, H. Kanda, and T. Notomi, "Loop-mediated isothermal amplification (lamp) of gene sequences and simple visual detection of products," *Nature protocols*, vol. 3, no. 5, pp. 877–882, 2008.
- [8] M. Nimesh, D. Joon, M. Varma-Basil, and D. Saluja, "Development and clinical evaluation of sdaa loop-mediated isothermal amplification assay for detection of mycobacterium tuberculosis with an approach to prevent carryover contamination," *Journal of clinical microbiology*, vol. 52, no. 7, pp. 2662–2664, 2014.
- [9] E.-J. Kil, S. Kim, Y.-J. Lee, E.-H. Kang, M. Lee, S.-H. Cho, M.-K. Kim, K.-Y. Lee, N.-Y. Heo, H.-S. Choi *et al.*, "Advanced loop-mediated isothermal amplification method for sensitive and specific detection of tomato chlorosis virus using a uracil dna glycosylase to control carry-over contamination," *Journal of virological methods*, vol. 213, pp. 68–74, 2015.
- [10] E.-M. Kim, H.-S. Jeon, J.-J. Kim, Y.-K. Shin, Y.-J. Lee, S.-G. Yeo, and C.-K. Park, "Uracil n-glycosylase-treated reverse transcription loop-mediated isothermal amplification for rapid detection of avian influenza virus preventing carry-over contamination," *Journal of veterinary science*, 2015.
- [11] M. Donolato, E. Sogne, B. T. Dalslet, M. Cantoni, D. Petti, J. Cao, F. Cardoso, S. Cardoso, P. Freitas, M. F. Hansen *et al.*, "On-chip measurement of the brownian relaxation frequency of magnetic beads using magnetic tunneling junctions," *Applied Physics Letters*, vol. 98, no. 7, p. 073702, 2011.
- [12] J. Ducrée, S. Haerberle, S. Lutz, S. Pausch, F. Von Stetten, and R. Zengerle, "The centrifugal microfluidic bio-disk platform," *Journal of Micromechanics and Microengineering*, vol. 17, no. 7, p. S103, 2007.
- [13] R. Gorkin, J. Park, J. Siegrist, M. Amasia, B. S. Lee, J.-M. Park, J. Kim, H. Kim, M. Madou, and Y.-K. Cho, "Centrifugal microfluidics for biomedical applications," *Lab on a Chip*, vol. 10, no. 14, pp. 1758–1773, 2010.
- [14] Y.-L. Lau, M.-Y. Lai, B.-T. Teoh, J. Abd-Jamil, J. Johari, S.-S. Sam, K.-K. Tan, and S. AbuBakar, "Colorimetric detection of dengue by single tube reverse-transcription-loop-mediated isothermal amplification," *PLoS one*, vol. 10, no. 9, p. e0138694, 2015.
- [15] J. Song, M. G. Mauk, B. A. Hackett, S. Cherry, H. H. Bau, and C. Liu, "Instrument-free point-of-care molecular detection of zika virus," *Analytical Chemistry*, vol. 88, no. 14, pp. 7289–7294, 2016.
- [16] M. Donolato, P. Antunes, R. S. Bejhed, T. Zardan Gomez de la Torre, F. W. Østerberg, M. Stromberg, M. Nilsson, M. Strømme, P. Svedlinth, M. F. Hansen *et al.*, "Novel readout method for molecular diagnostic assays based on optical measurements of magnetic nanobead dynamics," *Analytical chemistry*, vol. 87, no. 3, pp. 1622–1629, 2015.
- [17] K. Hsieh, P. L. Mage, A. T. Csordas, M. Eisenstein, and H. T. Soh, "Simultaneous elimination of carryover contamination and detection of dna with uracil-dna-glycosylase-supplemented loop-mediated isothermal amplification (udg-lamp)," *Chemical Communications*, vol. 50, no. 28, pp. 3747–3749, 2014.